Varying roles of ENSO and SAM on the Antarctic Peninsula climate in austral spring

Kyle R. Clem[1] and Ryan L. Fogt[1]

Received 25 June 2013; revised 18 September 2013; accepted 18 September 2013; published 18 October 2013.

[1] Recent studies have identified a significant warming trend across West Antarctica and the Antarctic Peninsula, which is likely linked to tropical forcing. Here we investigate temporal variations in El Niño–Southern Oscillation (ENSO)–related tropical forcing and Southern Annular Mode (SAM)–related forcing on the Amundsen-Bellingshausen Seas Low and the regional climate during austral spring. We find a spatial dependency regarding the impacts each of these climate modes have on the Antarctic Peninsula: relationships with ENSO and Antarctic Peninsula climate are persistent and significant across the western Peninsula, while relationships with the SAM are persistent and significant across the northeastern Peninsula. Other ENSO/SAM–Peninsula temperature correlations appear weak since 1957 as they vary temporally, fluctuating in response to changing correlations between the SAM index and the Southern Oscillation Index in austral spring. Changes in the ENSO-SAM correlations are due primarily to the 1988 La Niña/SAM negative event, which significantly altered the location of the ENSO teleconnection in the South Pacific Ocean and, therefore, its influence on the regional climate. Whether or not there is decadal variability in the ENSO-SAM relationship remains unclear; however, it is evident that the influence across the Peninsula varies in both space and time, related to the strength and spatial extent of the response in the Amundsen-Bellingshausen Seas. This suggests that in order to accurately attribute the warming to ENSO-related tropical forcing, it is necessary to consider the role of the regional circulation manifested by the phase of each climate mode together.

Citation: Clem, K. R., and R. L. Fogt (2013), Varying roles of ENSO and SAM on the Antarctic Peninsula climate in austral spring, *J. Geophys. Res. Atmos.*, *118*, 11,481–11,492, doi:10.1002/jgrd.50860.

1. Introduction

[2] Over the last 4 years, studies have detailed statistically significant warming since 1957 encompassing both the Antarctic Peninsula and West Antarctica [*Steig et al.*, 2009; *O'Donnell et al.*, 2011; *Bromwich et al.*, 2013]. While there are differences in the magnitude of the trends, these studies agree that the warming is most marked in West Antarctica during the austral spring (September–November, hereafter SON) and the Antarctic Peninsula during the austral winter [June–August (JJA)]. Consistent with the warming trends are changes in the sea ice concentration in the nearby Amundsen-Bellingshausen Seas, specifically a decrease in the sea ice season [*Stammerjohn et al.*, 2008, 2012] and an overall decrease in the sea ice concentration and extent [*Comiso*, 2010; *Massom et al.*, 2012]. Possibly tied to the warming, in addition to the flux of circumpolar deep water and changes in the nearshore wind field [*Steig et al.*, 2012], is the acceleration of outlet glaciers in the Amundsen Sea embayment, namely, the Pine Island and Thwaites Glaciers [*Rignot*, 2001; *Joughin et al.*, 2003].

[3] Recent analyses have pointed to the important role that forcing from the tropics plays in changing the regional atmospheric circulation and accelerating the warming, particularly from West Antarctica to the Antarctic Peninsula [*Schneider and Steig*, 2008; *Ding et al.*, 2011; *Schneider et al.*, 2012a, 2012b; *Ding and Steig*, 2013]. Most recently, *Ding and Steig* [2013] have demonstrated that widespread warming across the Antarctic Peninsula in austral fall is related to tropical sea surface temperature variability; they have also suggested that warming in the following austral winter and spring is due to the persistence of anomalous sea ice conditions from austral fall. Although not tied to tropical forcing explicitly, *Fogt et al.* [2012a] found a connection with increasing strength of cyclones in the Ross Sea in SON, which enhances warm air advection onto West Antarctica and is consistent with the warming trends being most marked in this season. These cyclones, as well as those in the Amundsen and Bellingshausen Seas, are strongly tied to the magnitude and location of the climatological low-pressure feature in the region, namely, the Amundsen-Bellingshausen Seas Low (ABSL) [*Fogt et al.*, 2012a; *Turner et al.*, 2013; *Hosking et al.*, 2013].

[4] Several studies note temporal variability in the tropically driven response across the South Pacific, particularly when considering teleconnections arising from the El

[1]Scalia Laboratory for Atmospheric Analysis and Department of Geography, Ohio University, Athens, Ohio, USA.

Corresponding author: K. R. Clem, Scalia Laboratory for Atmospheric Analysis and Department of Geography, Ohio University, Athens, OH 45701, USA. (kc268406@ohio.edu)

2169-897X/13/10.1002/jgrd.50860

Table 1. Antarctic Peninsula Stations Used in the Study[a]

Station	Latitude (°S)	Longitude (°W)	Starting Year	Percent Complete
Bellingshausen	−62.2	−58.9	1968	100
Esperanza	−63.4	−57.0	1945	96.4
Faraday/ Vernadsky	−65.4	−64.4	1950	100
Marambio	−64.2	−56.7	1970	98.4
Rothera	−67.5	−68.1	1977	100

[a]The starting year and percent complete refer to the surface temperature records in austral spring. Most other meteorological variables have the same starting date and completeness.

Niño–Southern Oscillation (ENSO) [*Kwok and Comiso*, 2002; *Silvestri and Vera*, 2003; *Turner*, 2004; *Carvalho et al.*, 2005; *Lachlan-Cope and Connolley*, 2006; *Gregory and Noone*, 2008; *Fogt and Bromwich*, 2006; *Fogt et al.*, 2011]. In particular, *Fogt et al.* [2011] found that the strength of the ENSO teleconnection to the South Pacific is governed by the coupling of ENSO with the Southern Annular Mode (SAM), a climate pattern representing the strength of the meridional pressure gradient across the extratropical Southern Hemisphere. When an El Niño (La Niña) event occurs with a negative (positive) SAM event, the two climate patterns are said to be "in phase", and the ENSO teleconnection to the South Pacific is stronger than average. *Fogt et al.* [2011] also noted that when ENSO and SAM are "out of phase" [when an El Niño (La Niña) event occurs with a positive (negative) SAM event], the teleconnection is significantly weakened, displaced, or altogether absent. Using this ENSO-SAM relationship, *Fogt and Bromwich* [2006] determined that the overall weak ENSO teleconnection to the South Pacific in SON during the 1980s was due to a negative correlation between the Southern Oscillation Index (SOI) and the SAM index, indicating an out-of-phase relationship between these two modes. In the 1990s, the correlation became significantly positive, and as a result, the teleconnection was amplified. Several studies have found that the combination of SAM and ENSO events plays a role in the season length, extent, and interannual variability of Antarctic sea ice in the Amundsen, Bellingshausen, and Weddell Seas [*Yuan*, 2004; *Stammerjohn et al.*, 2008].

[5] The preference for SAM positive phases to occur during La Niña events and for SAM negative phases to occur during El Niño events (the in-phase relationship described above) has been investigated by several studies [*L'Heureux and Thompson*, 2006; *Fogt et al.*, 2011; *Gong et al.*, 2010, 2013; *Ding et al.*, 2012]. These papers point to the anomalous flux of (transient) wave activity in the tropical Pacific during La Niña events that generates strong anticyclonic wave breaking on the equatorward side of the midlatitude jet. The increase in synoptic-scale anticyclonic wave breaking, in turn, generates zonal wind anomalies that maintain the low-pressure anomalies poleward of 60°S associated with the positive SAM phases; opposite conditions are observed during El Niño events, which preferentially create high-latitude positive pressure anomalies and negative SAM phases. More recently, *Gong et al.* [2013] have used an idealized general circulation model and have found that it is the degree of zonal symmetry in tropical heating that leads to the frequency and preference of in-phase ENSO-SAM combinations. In a similar vein, *Ding et al.* [2012] suggested there are two dynamical aspects of the SAM, one which is internally dynamically driven and more zonally symmetric across the Indian Ocean and another that is more strongly zonally asymmetric across the Pacific and forced from Rossby waves emanating from the tropics. The findings of *Ding et al.* [2012] are consistent with *Fogt et al.* [2012b], who note that the asymmetric SAM structure in the Pacific is primarily due to tropical activity.

[6] Given the important SAM-ENSO relationships, this study builds upon these earlier works by examining the role of ENSO and SAM on the Antarctic Peninsula climate in further detail. Our focus is on the Antarctic Peninsula rather than West Antarctica due to longer and more reliable station observations and because we find the relationships to be the strongest there. Furthermore, we also examine the influence of a particularly strong La Niña/SAM negative event during SON 1988. This event not only generates the apparent decadal ENSO-SAM correlation sign change from the 1980s to the 1990s noted by *Fogt and Bromwich* [2006] but also strongly modulates the climate of the Antarctic Peninsula compared to typical La Niña events. The paper is laid out as follows: section 2 briefly describes the data and methods, and section 3 presents our key findings. A summary and conclusions are offered in section 4.

2. Data and Methods

[7] ENSO activity is monitored using the Southern Oscillation Index (SOI) obtained from the Climate Prediction Center (CPC, www.cpc.noaa.gov). For SAM events, we use the observation-based index of *Marshall* [2003]. It should be noted that the key findings presented here are not sensitive to the ENSO or SAM index employed; similar results are obtained using either the Niño 3.4 region sea surface temperature anomalies or the U.S. Climate Prediction Center's Antarctic Oscillation index for defining the SAM (which is based on the leading empirical orthogonal function of 700 hPa geopotential height poleward of 20°S). We investigate these relationships through correlation analysis and anomaly composites of the atmospheric circulation. The temporal variability of the ENSO teleconnection and its impacts on the Antarctic Peninsula climate are detected as in *Fogt and Bromwich* [2006] using 10 year running correlations, as this method displays significant shifts in the ENSO-SAM relationship during SON. The sensitivity to this approach is addressed later in the manuscript; however, qualitatively similar results are obtained using 15 year running correlations.

[8] Similar to *Fogt et al.* [2012a], the variations in the ABSL central pressure are defined using the monthly minimum reanalysis sea level pressure value in the region 55–75°S, 180–60°W. To describe this feature and the atmospheric circulation, various parameters from the European Centre for Medium-Range Weather Forecasts (ECMWF) Interim reanalysis (hereafter ERA-Int) [*Dee et al.*, 2011] at 1.5° × 1.5° latitude-longitude resolution are employed, starting in 1979; similar results are obtained with other resolutions of ERA-Int and with other contemporary reanalyses. For Antarctic Peninsula meteorological data, we use the quality-controlled online Reference Antarctic Data for Environmental Research archive [*Turner et al.*, 2004] at five stations with nearly complete records spanning over 30 years. Information on these stations is included in Table 1, and they are displayed (along with the ABSL region) in Figure 1. With regard to the

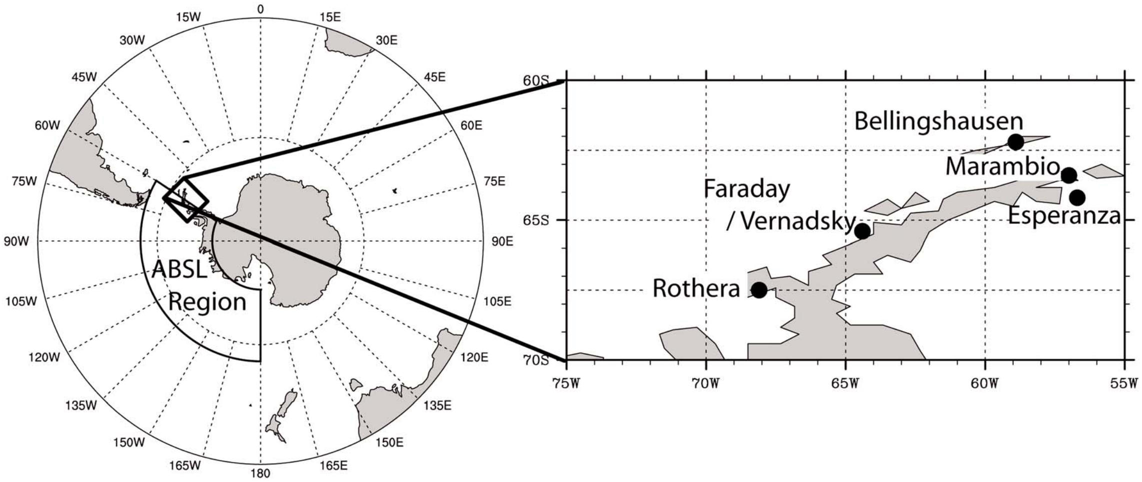

Figure 1. Map showing the locations of the ABSL region and the Antarctic Peninsula stations used in the study.

station locations, it should be noted that Rothera and Faraday stations are located on the western side of the Antarctic Peninsula, Bellingshausen is located on the northern tip of the Peninsula, and Marambio and Esperanza are located on the northeastern side of the Peninsula. The period of study is from 1957 to 2012, with the climatological reference period defined as 1981–2010.

3. Results

3.1. Antarctic Peninsula Temperature Correlations and Regressions

[9] Table 2 presents seasonal detrended correlations between surface temperatures at the five selected Antarctic Peninsula stations and the SOI and the *Marshall* [2003] SAM index over the full period of record. To assess the relative roles of ENSO and SAM on the temperatures, regression coefficients (also based on detrended data) and their 95% confidence intervals are displayed in Table 3. The SAM index has a relatively persistent, dominant, and statistically significant ($p < 0.05$) influence across all seasons with the Antarctic Peninsula temperatures, except for the western Peninsula stations (i.e., Rothera and Faraday). Although the SAM index–temperature correlations are generally the weakest in austral spring, in austral summer, the SAM has the weakest influence on the magnitude of the interannual temperature fluctuations across all stations, based on the regression coefficients in Table 3. On the other hand, the ENSO relationship with Antarctic Peninsula temperatures, as measured by the temperature correlations and regressions with the SOI, is weaker and seasonally varying. The SOI correlations are strongest in austral spring, when the majority of the stations show a statistically significant relationship (at $p < 0.05$); in austral spring, the magnitude and significance of the SOI regression coefficients with the Antarctic Peninsula temperatures typically also reach their maximum (Table 3). As noted by *Marshall* [2007], during austral spring, there is a difference in correlations and regressions between stations located on the western Peninsula (hereafter Rothera and Faraday; see Figure 1 for locations) and those located on the northeast Peninsula (hereafter Marambio and Esperanza). Notably, the SAM index–temperature relationships in Tables 2 and 3 over the full period of record show the highest levels of statistical significance ($p < 0.01$) at the northeast Peninsula stations, while it is observed that significant ($p < 0.01$) SOI correlations are found along the western Peninsula stations, extending up to Bellingshausen (see Figure 1). Furthermore, based on the magnitude of the SON regression coefficients in Table 3, the SOI influence dominates the SAM influence across the western Peninsula, while the SAM influence dominates the SOI influence at the northeastern Peninsula in SON. While Esperanza shows a significant correlation with the SOI at $p < 0.05$, this correlation is only statistically significant at $p < 0.10$ with the Niño 3.4

Table 2. Seasonal Detrended Correlations of Antarctic Temperature Data With the SOI and the *Marshall* [2003] SAM Index Over the Full Period of Station Records (or 1957, Whichever Is Later) as Indicated in Table 1[a]

	DJF		MAM		JJA		SON	
Station	SOI	SAM	SOI	SAM	SOI	SAM	SOI	SAM
ABSL Pressure	**−0.42**	***−0.77***	−0.24	***−0.52***	**−0.36**	***−0.72***	−0.21	***−0.81***
Rothera	−0.12	−0.23	0.22	***0.50***	**0.35**	0.24	***0.52***	**0.36**
Faraday	0.04	**−0.27**	0.10	0.14	**0.28**	0.13	***0.55***	−0.14
Bellingshausen	0.04	**0.32**	0.18	***0.53***	0.08	***0.46***	***0.38***	**0.30**
Marambio	0.04	***0.39***	−0.07	***0.51***	0.06	***0.41***	0.20	***0.50***
Esperanza	0.06	***0.45***	0.03	***0.39***	0.05	***0.42***	**0.29**[b]	***0.36***

[a]The correlation of the minimum sea level pressure in the vicinity of the ABSL (55–75°S, 180–60°W; Figure 1) is also given. Boldface correlations are significantly different from zero at $p < 0.05$; boldface and italicized correlations are significantly different from zero at $p < 0.01$.

[b]The detrended correlation with Esperanza temperatures and the Niño 3.4 sea surface temperatures is significant only at $p < 0.10$.

Table 3. As in Table 2 but for Seasonal Detrended Regression Coefficients (Units of °C/Standardized Index for Antarctic Peninsula Temperatures and hPa/Standardized Index for the ABSL Minimum) and 95% Confidence Intervals[a]

Station	DJF		MAM		JJA		SON	
	SOI	SAM	SOI	SAM	SOI	SAM	SOI	SAM
ABSL pressure	**−1.40 ± 1.08**	***−2.61 ± 0.79***	−0.72 ± 1.04	***−1.68 ± 0.99***	**−1.61 ± 1.49**	***−2.94 ± 1.04***	−0.79 ± 1.36	***−3.02 ± 0.80***
Rothera	−0.07 ± 0.20	−0.14 ± 0.21	0.26 ± 0.42	***0.66 ± 0.40***	**0.96 ± 0.90**	0.62 ± 0.89	***0.87 ± 0.50***	**0.59 ± 0.54**
Faraday	0.03 ± 0.19	**−0.16 ± 0.15**	0.14 ± 0.36	0.19 ± 0.37	**0.75 ± 0.70**	0.32 ± 0.65	***0.83 ± 0.34***	−0.22 ± 0.41
Bellingshausen	0.02 ± 0.16	**0.16 ± 0.15**	0.17 ± 0.30	***0.57 ± 0.28***	0.14 ± 0.57	***0.86 ± 0.51***	***0.34 ± 0.25***	**0.28 ± 0.28**
Marambio	0.04 ± 0.29	***0.37 ± 0.27***	−0.18 ± 0.75	***1.36 ± 0.72***	0.16 ± 0.81	***1.07 ± 0.75***	0.37 ± 0.57	***1.04 ± 0.56***
Esperanza	0.06 ± 0.25	***0.35 ± 0.19***	0.07 ± 0.58	***0.85 ± 0.55***	0.11 ± 0.61	***0.85 ± 0.49***	**0.45 ± 0.41**	***0.57 ± 0.41***

[a]Statistical significance is as denoted in Table 2.

sea surface temperatures and is the weakest (in terms of magnitude) of all the statistically significant correlations in SON. As a result, the ENSO influence on Esperanza temperatures, and undoubtedly Marambio temperatures, is much weaker than with temperatures along the western Antarctic Peninsula. Although the varying roles of ENSO and SAM across the Antarctic Peninsula in SON are also observed in June–August (JJA), the statistical significance of the SOI relationships across the western Antarctic Peninsula is much stronger in SON (Tables 2 and 3); the JJA SOI relationships are barely significant at $p < 0.05$ and are not significant in the original (with trend) data at Faraday. Therefore, SON is the focus for the remainder of the paper.

3.2. Connections to the ENSO-SAM Relationship

[10] As noted by *Fogt and Bromwich* [2006], the variability of the ENSO teleconnection to the high-latitude South Pacific fluctuates in time, and therefore, significant correlations may exist on shorter time scales. Other studies have similarly noted nonstationary impacts of the SAM, such as with temperatures at Halley station in Antarctica [*Marshall et al*., 2011] or with precipitation and moisture convergence over southern South America [*Silvestri and Vera*, 2003, 2009]. To investigate these time dependencies, we plot in Figure 2 the 10 year running correlations between the Antarctic Peninsula temperatures and the SOI and the SAM index. Based on the analysis presented in Table 2, it is expected that a persistent correlation exists between the SAM index and temperature along the northeastern Peninsula (Marambio and Esperanza) and the SOI and temperature along the western Peninsula (Rothera and Faraday). These running correlations that are expected to be persistent in time are plotted separately in Figure 2a, and although small fluctuations exist depending on the 10 year period, the correlation sign and magnitude between the SOI and western Peninsula temperatures and the SAM and northeastern Peninsula temperatures remain nearly the same over the full period of record at each station. The only exception to this is Esperanza, where the SAM-temperature correlation starts out negative but quickly switches to a positive correlation after 1970 and remains positive through 2012. This switch of the correlation at Esperanza at 1970 will be discussed in more detail later. Therefore, Figure 2a reveals that the long-term

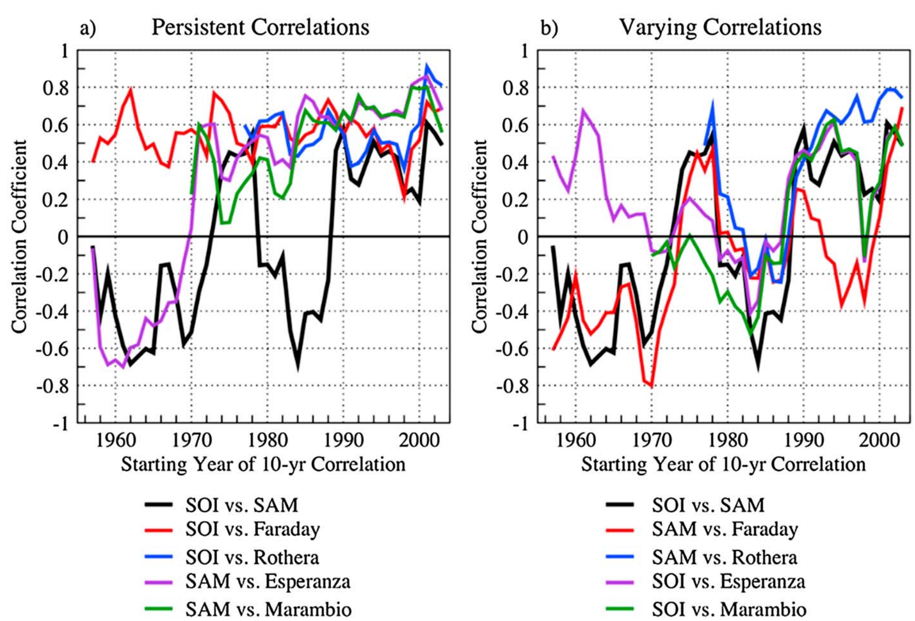

Figure 2. Running SON decadal correlations (i.e., 1980 represents the 1980–1989 10 year correlation) for (a) persistent correlations between the SOI and the SAM index with Antarctic Peninsula temperatures and (b) time-varying correlations between the SOI and the SAM index with Antarctic Peninsula temperatures. In both Figures 2a and 2b, the SON decadal correlation between the SOI and the SAM index is plotted as a solid black line.

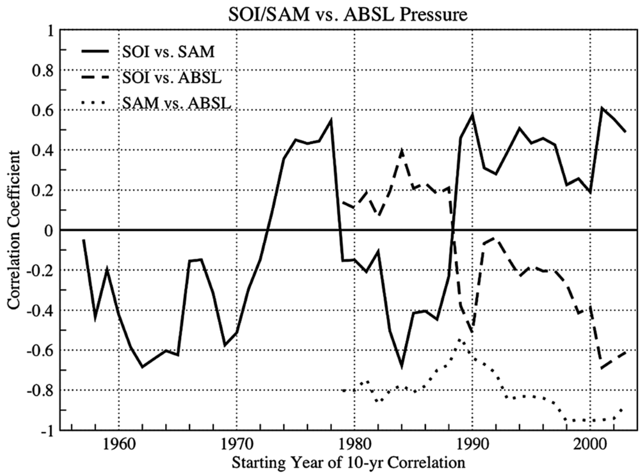

Figure 3. Running SON decadal correlations for the SOI and the SAM index with the ABSL minimum central pressure.

statistically significant correlations during SON (Table 2) are composed of persistent correlations on decadal time scales.

[11] From Table 2, the correlations which were identified as not statistically significant at $p < 0.01$ over the full period of record show marked changes in the sign and magnitude of the 10 year running correlations (Figure 2b). In most cases, the correlations are of one sign during much of the 1970s, switch sign during the 1980s, and then reverse again during the 1990s–2000s. While this relationship weakens slightly at Faraday during the 1990s, it is found to be strong for all other decades over its period of record. Most interesting is that the temporal changes in correlation between the SAM index and temperatures on the western Peninsula and the SOI and temperatures on the northeast Peninsula nearly trace the changes in the SOI–SAM index correlation during austral spring (shown as a solid black line in Figure 2). In other words, both the SAM relationship with western Peninsula temperatures and the ENSO relationship with the northeastern Peninsula temperatures are related to the ENSO-SAM relationship. The temporally varying correlations that follow the SOI–SAM index correlation in Figure 2b are in contrast with the persistent correlations in Figure 2a, demonstrating that the ENSO- and SAM-related impacts on Antarctic Peninsula temperatures vary spatially.

[12] Also noteworthy from Figure 2 is that the 1960s and the 1980s are dominated by a negative SOI–SAM index correlation, while the 1970s are marked with a brief positive correlation. Near 1990, a rapid switch from a negative to a positive correlation arises, and the positive correlation persists through both the 1990s and the 2000s. Similar correlation sign switches, albeit weaker in magnitude, are also observed using 15 year running correlations during the 1957–2012 period. While the change in the SOI–SAM index correlation between the 1980s and the 1990s was noted by *Fogt and Bromwich* [2006], their study only extended to 2001; the persistence of the in-phase relationship through 2002–2012 and other previous correlation sign switches prior to 1980 extends their work. The correspondence of the temporally varying correlations in Figure 2b with the SOI–SAM index correlations changes is robust, as not only are changes in the sign of these correlations reflected by the SOI–SAM index correlation, but the magnitude of the correlations is also nearly the same throughout the 50+ year record. The SAM index–temperature relationship is particularly strong at Faraday, and the brief break in its relationship with the SOI–SAM index correlation in the 1990s is strongly overshadowed by the otherwise tracing of the correlations during all other decades.

[13] For Esperanza, the switch in behavior of the SAM index–temperature correlation before and after 1970 alluded to earlier is also observed in its decadal correlations with the SOI (Figure 2b). Before 1970, the SOI–Esperanza temperature correlation mirrored the SOI–SAM index correlation, while the SAM–Esperanza temperature correlation traced the SOI–SAM index correlation. After 1970, the correlations switch, and the behavior is the same as at Marambio and described previously. These changes in the SAM and ENSO correlations with Esperanza temperatures highlight similar variability as the SOI–SAM index correlation, albeit with a switch around 1970 for reasons unknown.

[14] Altogether, Figure 2 suggests that the influence of SAM on the western Peninsula climate and that of ENSO on the northeastern Peninsula climate are strongly modulated by the relationship between ENSO and SAM events, including temporal fluctuations in this relationship. Furthermore, other climate parameters [such as wind speed, mean sea level pressure (MSLP), and meridional wind] also show a strong linear relationship that varies in time in accordance with the SOI–SAM index correlation.

[15] Why are there differences between the relationship of ENSO and SAM on the northeastern and western Peninsula climate? From Figure 2, it is apparent that the temperature impacts across the Peninsula are at least partly driven by the temporally changing relationship between ENSO and SAM. As noted previously, *Fogt and Bromwich* [2006] found that the variations in the South Pacific ENSO teleconnection between the 1980s and the 1990s in austral spring are strongly influenced by the relationship between ENSO and SAM. The influence of the South Pacific ENSO teleconnection is examined further in Figure 3 using the minimum pressure in the vicinity of the ABSL (as employed in *Fogt et al*. [2012a] and *Turner et al*. [2013]), where the 10 year running SOI–SAM index correlations from Figure 2 are plotted alongside the 10 year running correlations of the SOI (dashed line) and the SAM index (dotted line) with the ABSL minimum central pressure. Despite an overall weak correlation between the SOI and the ABSL central pressure (Table 2), it is readily apparent that there is a strong linear relationship between the running SOI–SAM index correlation and the SOI–ABSL central pressure running correlations: the SOI-ABSL and SOI–SAM index running correlations in Figure 3 nearly mirror each other from 1979 onward. In La Niña events (SOI > 0), for example, the positive SOI–ABSL central pressure correlation implies higher than normal ABSL central pressures (as in the 1980s, when the SOI–SAM index correlation is negative) and deeper than normal ABSL central pressures when the SOI–ABSL central pressure correlation is negative (as in the 1990s and the 2000s, when the SOI–SAM index correlation is positive). Similar extensions can be made to the time-varying correlations with the Antarctic Peninsula temperatures presented in Figure 2b. The fact that the running correlations mirror each other in Figure 3 strongly suggests that the ENSO influence on the ABSL is related to the phase of the SAM, implying that the location and/or magnitude of the ABSL changes during times

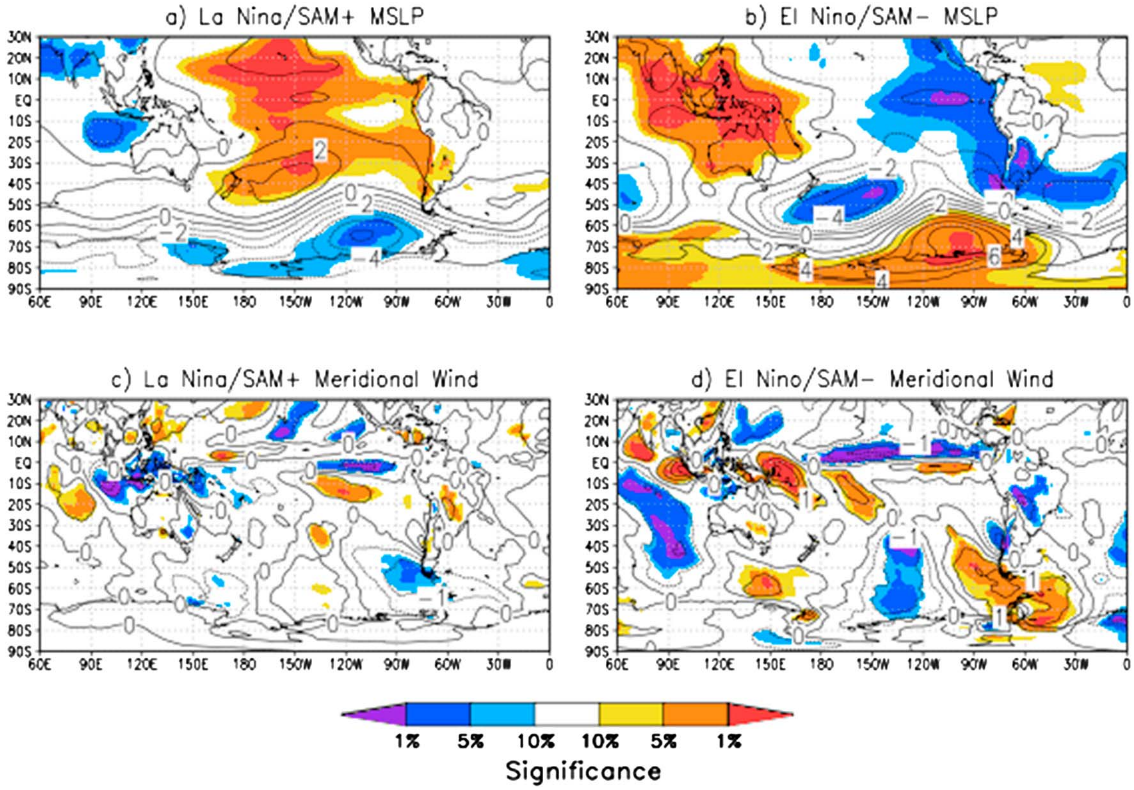

Figure 4. Anomaly composites of top simultaneous strong (top 70th percentile) in-phase ENSO and SAM austral spring events based on the ERA-Int reanalysis compared to the 1981–2010 climatology. Composites are for (a) La Niña/SAM+ MSLP, (b) El Niño/SAM− MSLP, (c) La Niña/SAM+ meridional wind, and (d) El Niño/SAM− meridional wind. Shading indicates anomalies statistically different from zero at $p < 0.10$, $p < 0.05$, and $p < 0.01$.

when ENSO events act in isolation compared to times when they occur with SAM events. In stark contrast, the SAM relationship with the ABSL central pressure (Figure 3) shows little variation throughout time and no linear relationship with the SOI–SAM index correlation; positive SAM events (for example) always deepen the pressures somewhere within the ABSL region. It should be noted that although the magnitude of the correlations changes when using the relative central pressure definition of the ABSL as outlined in *Hosking et al.* [2013], the ABSL pressure–SAM index running correlations still fluctuate independently of the SOI–SAM index running correlations, while the ABSL pressure–SOI correlations still fluctuate with the SOI–SAM index running correlations.

[16] Together, Figures 2 and 3 demonstrate both persistent (in time) significant correlations across the ABSL to the Antarctic Peninsula and time-varying correlations (generally weak and statistically insignificant over the full period of record) that fluctuate temporally with the ENSO-SAM relationship. Apparently, it is the changes in the circulation arising from the ENSO-SAM relationship that drive these time-varying influences across the Antarctic Peninsula through changes in the strength and position of the ABSL, given that the ABSL is the dominant and most persistent circulation feature of the region [*Fogt et al.*, 2012a; *Turner et al.*, 2013].

3.3. Atmospheric Circulation Composites

[17] To investigate these atmospheric circulation changes and their impacts on the Antarctic Peninsula, anomaly composites are used in two independent approaches. Since the time-varying influence of SAM on the western Peninsula and of ENSO on the northeastern Peninsula is linked to the relationship between ENSO and SAM, we first examine circulation anomalies associated with in-phase events (when a La Niña event occurs with a positive SAM or an El Niño event occurs with a negative SAM as in *Fogt et al.* [2011]). These events are based on years when both the SON SOI (and Niño 3.4 sea surface temperatures) and the SAM index exceed the 70th (fall below the 30th) percentile for both La Niña/SAM+ (El Niño/SAM−). These percentile thresholds were chosen to increase the sample size to four in-phase years in each composite and preserve a data set–independent match with both the SOI and Niño 3.4 sea surface temperatures. In all cases, anomaly composites are presented, and the statistical significance of the anomalies are tested against the null hypothesis of no change using a Student's *t* test. While *Fogt et al.* [2011] displayed composites across various ENSO and SAM events, our focus is only on austral spring and over a much smaller sample, thereby highlighting the influence of the strongest events.

[18] In-phase composites based on ERA-Int mean sea level pressure (MSLP) are shown in Figures 4a and 4b, and those based on for ERA-Int meridional wind are shown in Figures 4c and 4d. Readily apparent in the MSLP composites is the tropical ENSO signature, manifested as an east-west pressure difference across the tropical Pacific reminiscent of the Southern Oscillation (Figures 4a and 4b). Despite the

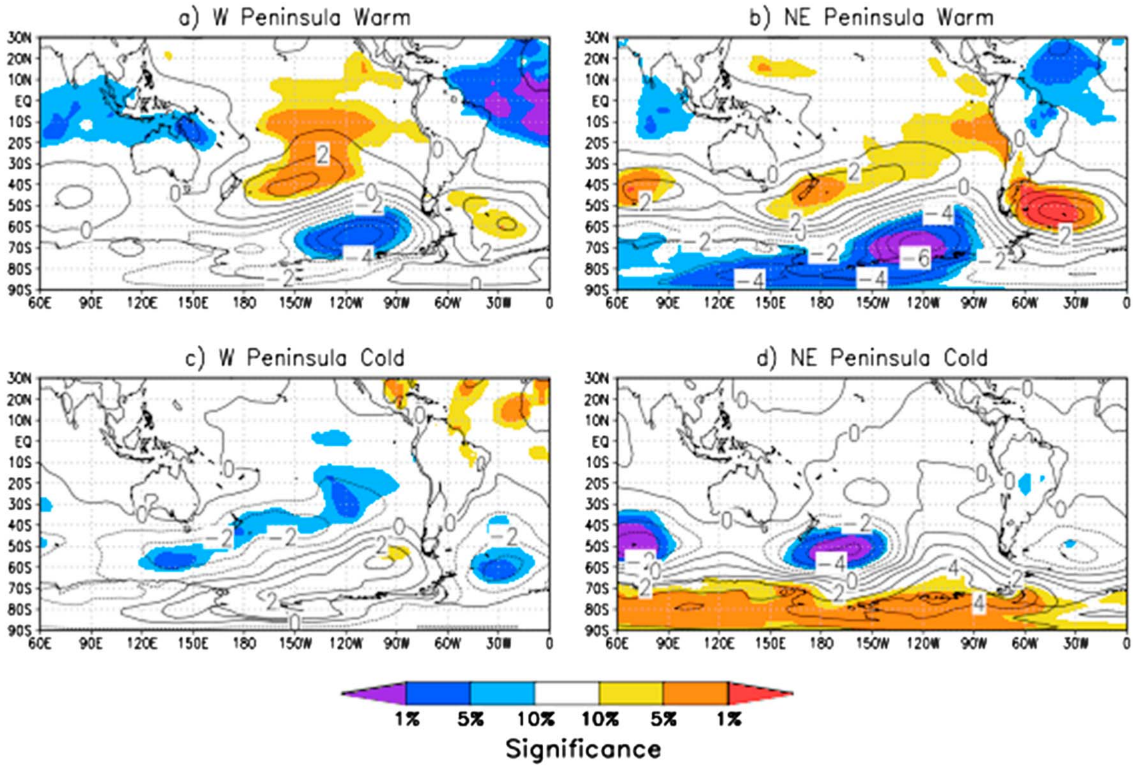

Figure 5. As in Figure 4 but for ERA-Int MSLP anomalies versus the 1981–2010 climatology during the top five highest (Warm) and lowest (Cold) spring temperatures across the Antarctic Peninsula. (a, c) The western Peninsula (W) consists of Rothera and Faraday stations. (b, d) The northeast Peninsula (NE) consists of Esperanza and Marambio stations.

simultaneous occurrence of SAM events, the only persistently marked circulation anomaly in the high southern latitudes is in the vicinity of the ABSL. During La Niña/SAM+ combinations in austral spring, the ABSL is more than 4 hPa below the climatological average (Figure 4a; significant at $p < 0.05$). The influence is especially marked for El Niño/SAM− cases, with pressure deviations more than 6 hPa above the climatological average, and significant at $p < 0.01$ (Figure 4b). As noted by *Fogt et al.* [2011], the simultaneous occurrence of in-phase ENSO and SAM events not only amplifies the typical ENSO signal in the South Pacific but also broadens its spatial extent. In particular, the broadening of the ABSL creates an influence on the meridional wind that extends from the western Peninsula to the northeast Peninsula (Figures 4c and 4d). Thus, the amplification and expansion of the ABSL anomalies, most marked during simultaneous in-phase ENSO and SAM events, allows for ENSO to have a pronounced influence on the northeastern Peninsula. The ENSO influence on this region is relatively weak and inconsistent otherwise [cf. *Fogt et al.*, 2011, Figures 5–8], thereby explaining the overall weak SOI–northeast Peninsula temperature correlations in Table 2 and the time-varying SOI–northeast Peninsula temperature correlations in Figure 2b.

[19] ENSO teleconnections to the South Pacific are also observed during times with weak or neutral SAM events [*Fogt et al.*, 2011], which explains the persistence of the SOI-temperature correlations on the western Antarctic Peninsula. In each of these cases (with or without SAM events), the flow around the anomalous circulation in the ABSL drives changes in the meridional wind that almost always extend across the western Peninsula. However, SAM events, which have a pronounced and persistent influence on temperatures across the northeastern Peninsula (Table 2 and Figure 2a) through Föhn effects [*Marshall et al.*, 2006; *Orr et al.*, 2008], have a weaker and time-varying response across the western Peninsula in austral spring. Similar to above, the broadening spatial extent of the ABSL is observed during in-phase SAM/ENSO events only; when SAM events occur without influence from ENSO, the response in the vicinity of the ABSL is often more zonally symmetric and confined much closer to the Antarctic continent [*Fogt et al.*, 2011, 2012b]. Although the SAM correlation with the ABSL minimum pressures remains persistent (Figure 3), the reduced spatial response in this region during SAM-only events (as compared to ENSO-only or in-phase events) produces flow that is not only weaker but also more zonal, with a less persistent impact on the temperatures across the western Peninsula. In turn, SAM index–temperature relationships across the western Peninsula vary in time, quite similarly as SOI-temperature correlations across the northeastern Peninsula vary in time. It can be thus inferred that these two time-varying relationships are strongly governed by the relationship between ENSO and SAM, through variations in both the intensity and spatial extent of the ABSL.

[20] Although La Niña conditions often occur with SAM positive events, and El Niño conditions often occur with SAM negative events [*Gong et al.*, 2010, 2013], thereby creating the circulation anomalies described in Figure 4, all phases of the SAM (including its neutral state) have been

Table 4. Years (in Rank Order) in SON Used to Create the Anomaly Composites for Figure 5[a]

West Peninsula				Northeast Peninsula			
Warm	ENSO-SAM Phase	Cold	ENSO-SAM Phase	Warm	ENSO-SAM Phase	Cold	ENSO-SAM Phase
2008	LN/SAM+	1982	EN/SAM−	2001	SAM+	1997	EN/SAM−
2010	LN/SAM+	1987	EN	2008	LN/SAM+	1980	SAM−
1989	neutral	1980	SAM−	2010	LN/SAM+	1994	EN/SAM−
1985	SAM+	1981	neutral	2005	LN	2007	LN/SAM−
1988	LN/SAM−	1986	EN/SAM+	1985	SAM+	2012	neutral

[a]The phases are based on when the climate index (SAM index and either the SOI or Niño 3.4 sea surface temperatures) is below or above the 30th or the 70th percentile, respectively. LN = La Niña; EN = El Niño.

observed during ENSO events in austral spring since 1957. In light of this, and to provide further evidence that the SAM-ENSO relationship plays a leading role in explaining temperature variations across the Peninsula, anomaly composites based on temperature records are presented in Figure 5. This approach provides an independent investigation on the atmospheric conditions driving temperature variations across the Peninsula, as the years included in these composites are derived solely from averaged temperature records on the western and northeastern Peninsula rather than from a climate pattern. For each case, the top five warmest and coldest SON years (approximately the 85th and 15th percentiles, respectively) of the averaged temperature records post 1979 were selected for compositing the circulation patterns; these years, along with the corresponding ENSO and SAM phases, are listed in Table 4. Consistent with our discussion, none of the warmest (coldest) years on the western Peninsula are El Niño (La Niña) events, and none of the warmest (coldest) years are SAM− (SAM+) for the northeastern Peninsula. In addition, for the northeastern Peninsula, the majority of the ENSO influence on the warm and cold years occurs during in-phase events, suggesting that these conditions have the dominant influence on temperatures across the region as outlined in Figure 4; otherwise, more than half of the years included in Figures 4 and 5 are different.

[21] Figure 5 shows the marked circulation differences between the western and northeastern Peninsula during warm and cold events. For the western Peninsula (Figures 5a and 5c), much of the anomalous circulation resembles a propagating Rossby wave emanating from the tropical Pacific, reminiscent of the Pacific South American pattern [*Karoly*, 1989; *Mo and Higgins*, 1998; *Mo and Paegle*, 2001] commonly observed during ENSO years. For the warm events (Figure 5a), below normal pressure anomalies ($p < 0.05$) are observed in the ABSL region, resulting in a more northerly flow across the western Peninsula generating above normal temperatures. During cold years (Figure 5c), the juxtaposition of the above normal pressure anomalies in the ABSL region and the below normal pressure anomalies ($p < 0.05$) in the Weddell Sea drive a more southerly flow along the western Peninsula, again strongly resembling a tropical wave train pressure pattern and little resemblance to a typical SAM pattern. Across the northeastern Peninsula (Figures 5b and 5d), there is a less marked tropical component to the circulation anomalies; instead, the anomalous circulation is more related to the SAM, with pressure anomalies significant at $p < 0.05$ observed inland across the Antarctic continent and within the ABSL region. This is consistent with a more persistent SAM influence on temperatures across the northeast Peninsula (Figure 2a and Tables 2 and 3) and on the ABSL (Figure 3). However, given that these temperatures are the most extreme cases, a slight tropical component to the regional circulation is still noted, which would be expected as it would further enhance the meridional flow across the region generating more extreme anomalous temperature events.

3.4. The 1988 La Niña/SAM Negative Event

[22] Until this point, the analyses detailing shifts in the SAM-ENSO relationship and the relationship these climate modes have with the Antarctic Peninsula climate have been based on running 10 year correlations. Due to the small sample size, 10 year correlations can be strongly influenced by the presence of outliers. Although similar (albeit weaker) shifts in the correlations are obtained using 15 year running windows, the sensitivity to outliers is still examined by removing individual SON years for the SOI and the SAM index and recalculating the running correlations. In performing these tests, it was noted that only the removal of the year 1988 had any significant influence on the running SOI–SAM index correlation sign; the correlations and their temporal changes remained robust otherwise. The SOI–SAM index running correlation when 1988 (which was characterized with a strong La Niña event and a very strong negative SAM event) is removed is depicted in Figure 6. Notably, with the removal of this event, the SOI–SAM index running correlation remains positive after the mid-1970s, consistent with the persistent positive correlation observed during austral summer

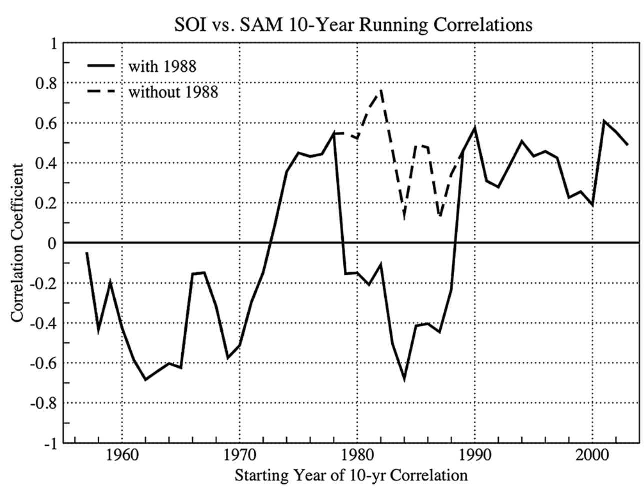

Figure 6. SON decadal running correlation between the SOI and the SAM index with and without the 1988 La Niña/SAM negative event.

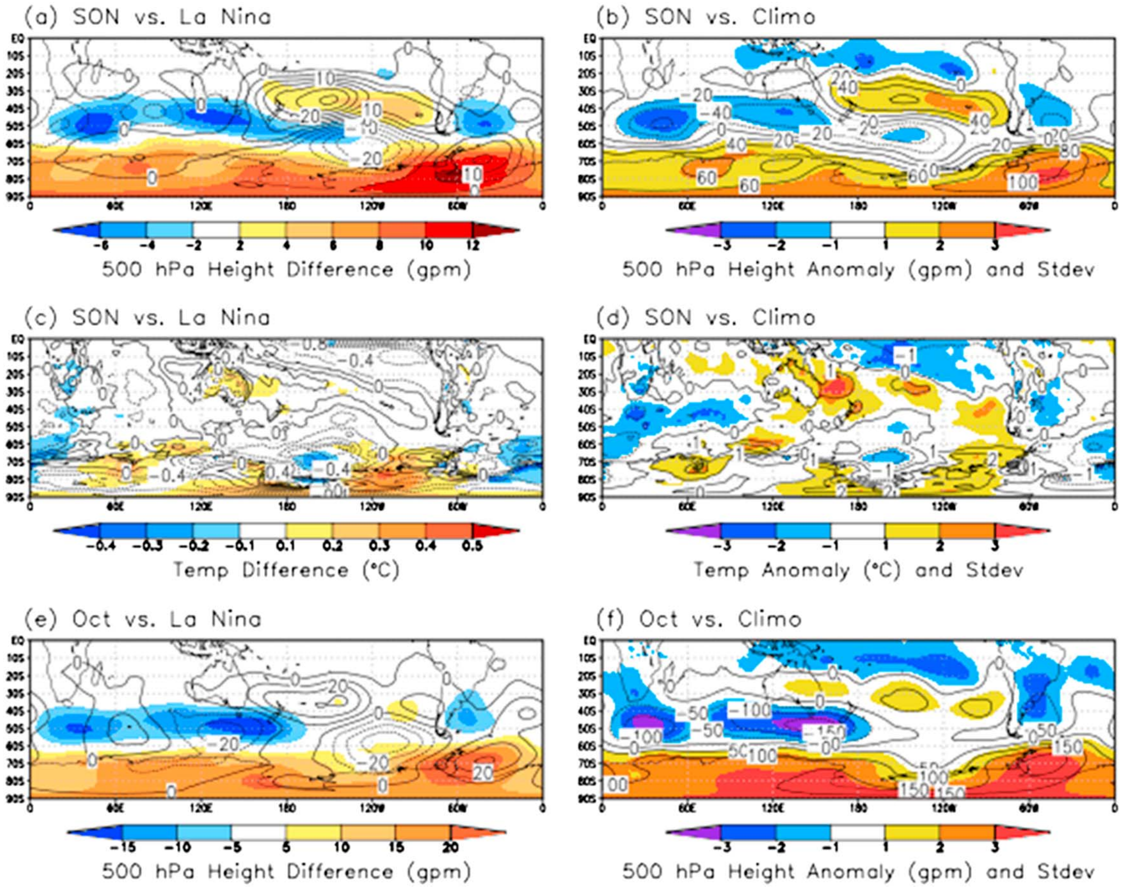

Figure 7. ERA-Int 1988 SON La Niña/SAM− event compared to (left) La Niña years (La Niña conditions contoured and 1988 anomalies shaded) and (right) the 1981–2010 climatology (anomalies contoured and standard deviations from climatology shaded) for (a–d) SON and (e, f) October 1988 only. Figures 7a, 7b, 7e, and 7f depict 500 hPa height. Figures 7c and 7d depict 2 m temperature. Nine La Niña events during SON identified by the CPC (1983, 1984, 1988, 1995, 1998, 1999, 2000, 2007, and 2010) were used in creating the composites for the left column.

[*L'Heureux and Thompson*, 2006; *Carvalho et al*., 2005; *Fogt and Bromwich*, 2006; *Fogt et al*., 2011]. In regard to Figure 2, the removal of 1988 does not significantly affect the conclusions made from the running correlations: although subtle differences are noted, in general, the persistent relationships observed in Figure 2a remain whether or not 1988 is included, while the time-varying relationships in Figure 2b still continue to trace the (revised) SOI–SAM index running correlation presented in Figure 6. Additionally, the removal of 1988 does not significantly alter the correlation/regression between the SOI and the SAM index over the full 1957–2012 period; the relationship remains weak and statistically insignificant, primarily due to the negative correlation prior to 1970 that reverses and remains positive after 1990 (Figures 2, 3, and 6).

[23] Given that 1988 produces a strong shift in the SON SOI–SAM index running correlation in the 1980s, it is prudent to examine the uniqueness of the circulation anomalies during this year. These plots are displayed in Figures 7a–7d, with comparisons made to La Niña events (including the 1988 La Niña event) in the left column and the 1981–2010 climatological SON mean in the right column. Figure 7a depicts the 500 hPa geopotential height composite mean La Niña conditions during SON (contours) and the 1988 differences from the La Niña mean (shaded); similar results are obtained using mean sea level pressure or other pressure levels in the troposphere. Typically, in a La Niña event (contours in Figure 7a), positive height anomalies ~10 geopotential meters (gpm) exist over the Weddell Sea, while negative height anomalies (~−20 gpm) are present in the Amundsen-Bellingshausen Seas and the broader South Pacific region. However, during the 1988 La Niña/SAM negative event, the positive height anomalies in the Weddell Sea are on the order of 10–12 gpm higher than normal La Niña conditions (shading in Figure 7a), giving rise to a positive geopotential height anomaly that is nearly double that observed during typical La Niña events. In contrast, in the South Pacific, the region of negative height anomalies normally seen during La Niña events is characterized by above (La Niña) average heights near the Antarctic Peninsula and lower than (La Niña) average heights northwest of this center. Effectively, this implies a reduction in the spatial extent of the ENSO teleconnection during the 1988 La Niña/SAM negative event, as it is shifted westward away from the Antarctic Peninsula toward the south central Pacific Ocean. These circulation changes are also depicted in Figure 7b: compared to the 1981–2010 climatological mean, the most negative height anomalies are found near 60°S, 150°W, which is much farther north and west than they are typically seen in La Niña conditions (contours in Figure 7a,

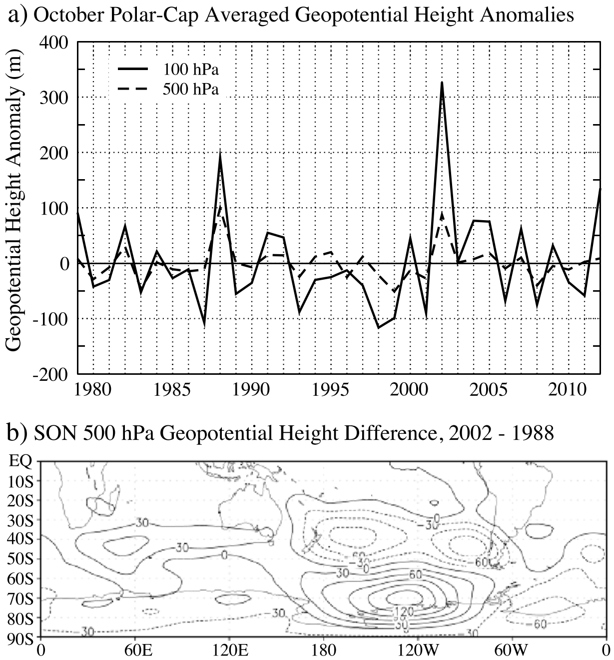

Figure 8. (a) October polar cap (60–90°S) geopotential height anomaly time series from ERA-Int at 100 hPa and 500 hPa. (b) SON geopotential height differences from 2002 and 1988. The contour interval is 30 m.

near 65°S, 120°W). Moreover, the above average heights in the Weddell Sea, which exceed 3 standard deviations from the climatological mean (Figure 7b), are a significant difference between this La Niña event and others during SON. These strong height anomalies are associated with both the SAM negative event and the northwestward displacement of the ENSO teleconnection in the high-latitude South Pacific (Figure 7a). As discussed in earlier studies [*L'Heureux and Thompson*, 2006; *Gong et al.*, 2010; *Fogt et al.*, 2011], it is the equatorward eddy momentum fluxes associated with the negative SAM event that oppose the poleward eddy momentum fluxes associated with La Niña events, disrupting the ENSO signal propagation to the high southern latitudes and displacing the teleconnection equatorward.

[24] The displacement of the ENSO teleconnection during SON 1988 is also clearly evident by the circulation changes and resulting temperature advection (through implied geostrophy). During typical La Niña events, above average temperatures are noted along coastal West Antarctica and the western Antarctic Peninsula (contours in Figure 7c). However, during the 1988 La Niña/SAM negative event, the strongest above normal temperature anomalies, indicated by the yellow and orange shading in Figure 7c, are located farther west and inland across interior West Antarctica (near ~80°S, 115°W). In addition, compared to other La Niña events, the maximum positive temperature anomalies (>1 standard deviation from the 1981 to 2010 climatological mean, Figure 7d) are displaced westward from the Antarctic Peninsula, which greatly reduces the impact across the northeast Peninsula, consistent with the change in correlation between SOI and northeast Peninsula temperatures in Figure 2b. The negative SAM event, which is typically marked with higher pressure in the Amundsen-Bellingshausen Seas, shows no discernable impact in this region due to the La Niña event. As such, the negative SAM influence on temperatures across the western Antarctic Peninsula is not as marked as it is across the northeast Peninsula, consistent with the change in this correlation observed in Figure 2b.

[25] A month-by-month investigation of the circulation anomalies associated with the 1988 La Niña/SAM negative event in SON reveals that the majority of the patterns displayed in Figures 7a–7d are strongly influenced by the conditions during October. During October 1988, the SAM reached an October record negative value (−6.03, for all Octobers over the period 1957–2012 based on the *Marshall* [2003] index) in conjunction with a moderately strong La Niña (SOI = +2.3). The October 1988 500 hPa geopotential height anomalies (Figures 7e–7f) are consistent with those depicted in Figures 7a and 7b, except that the above normal geopotential height anomalies in the Weddell Sea are further amplified while the ENSO teleconnection in the South Pacific is altogether absent. From Figure 7f, the Weddell Sea geopotential height anomalies exceed more than 3 standard deviations from the climatological mean over a much larger region than in Figure 7b. The circulation anomalies in Figure 7f clearly depict the strong SAM negative event; little indication of any La Niña pattern is discernable.

[26] The uniqueness of October 1988 is further displayed in Figure 8a, which shows the polar cap (60–90°S) averaged geopotential height anomalies in the stratosphere (100 hPa) and the lower troposphere (500 hPa, the first mandatory level above the high Antarctic interior). October 1988 was marked with the highest polar cap averaged 500 hPa geopotential heights since 1979 and the second highest at 100 hPa, with a strong positive height anomaly existing throughout the entire atmospheric column over Antarctica. The other similar year was 2002. Both 1988 and 2002 were characterized by strong stratospheric warming due to increased heat flux from tropospheric planetary waves [*Hio and Yoden*, 2005]. In 2002, the polar vortex split into two, an event that was not likely to have occurred since meteorological observations began over Antarctica in 1957 [*Roscoe et al.*, 2005], reflected here in Figure 8a with the record positive geopotential height anomaly at 100 hPa over the polar cap in 2002. Both of these years point to high southern latitude stratosphere-troposphere dynamics that influence the sign and magnitude of the SAM index, likely independently of ENSO activity. For the present study, the key delineator was that the negative SAM index in 1988 occurred with a La Niña event while the 2002 negative SAM event occurred during an El Niño event. Comparing the 500 hPa heights from 2002 and 1988 (Figure 8b) during SON, it is evident that the combination of El Niño/SAM negative conditions in 2002 produced much higher geopotential heights in the ABSL region (up to 150 m) than those observed during 1988 (in La Niña/SAM negative). In turn, the 1988 La Niña/SAM negative combination in austral spring gives rise to a negative correlation in the 1980s between the SOI and the SAM index (Figure 6); through the linear association with the SOI–SAM index correlation (Figure 2b), the negative SOI–SAM index correlation during the 1980s reduces the long-term correlation of SAM (ENSO) with the climate of the western (northeastern) Peninsula (Table 2).

[27] Despite this unique event in the 1980s, it is evident, simply based on the sign of the correlations presented in

Figure 2, that the SAM (ENSO) relationship with the western (northeastern) Antarctic Peninsula climate is dependent on the relationship between ENSO and SAM, especially since other negative SOI–SAM index correlations are observed prior to 1970. The in-phase combinations broaden the impacts of the ABSL, making the circulation anomalies (in particular, the meridional component to the circulation) extend across both the western and northeastern Peninsula. Otherwise, SAM events typically (but not necessarily always) only influence the northeastern Peninsula, while ENSO events typically influence the western Peninsula.

4. Summary and Conclusions

[28] Recent analyses have associated the ongoing warming in West Antarctica with forcing from the tropics [*Ding et al.*, 2011; *Schneider et al.*, 2012a, 2012b; *Bromwich et al.*, 2013]. The results presented here clearly demonstrate that variations in the ENSO-related tropical forcing to West Antarctica, specifically in the vicinity of the ABSL, are tied to variations in the SAM. We note that during austral spring, the ENSO relationship with the ABSL is linearly related to the SOI–SAM index correlation (or the degree to which these two climate patterns are “in phase”). In turn, changes in the SOI–SAM index relationship, through their impacts on the ABSL and/or the overall ENSO teleconnection, modulate the degree and sign of the ENSO influence on the northeastern Antarctic Peninsula climate and the SAM influence on the western Antarctic Peninsula climate. Using 10 year running correlations, there appears to be a sudden shift in the SOI–SAM index correlation, as noted by *Fogt and Bromwich* [2006], from the 1980s to the 1990s; however, this correlation shift is more likely a statistical artifact, influenced by the presence of a strong La Niña/SAM negative event in SON 1988. During this event, an unusually high (greater than 3 standard deviations from the climatological mean) pressure/height anomaly in the Weddell Sea, associated with the SAM negative event, hindered the propagation of the La Niña signal to the Amundsen-Bellingshausen Seas, displacing it farther north and west. This altered the ENSO impacts across the Antarctic Peninsula and West Antarctica. It is thus apparent that ENSO’s influence across West Antarctica and the Antarctic Peninsula, and therefore any influence it has on the warming in this region, is tied to the strength and phase of the SAM. Similarly, SAM-related impacts across the western Peninsula primarily depend on the phase of ENSO.

[29] Future work includes investigating the role of the position and intensity of tropical convection in generating variations in the ENSO-related Rossby waves and not only how this influences not only the overall ENSO teleconnection (as in *Lachlan-Cope and Connolley* [2006]) but also how they might influence the SAM phase [*Gong et al.*, 2010, 2013; *Ding et al.*, 2012]. Sea ice conditions, including their long-term trends, also deserve further investigation as they may play a role in the ENSO and SAM signatures in the Amundsen-Bellingshausen Seas through changes in surface sensible and latent heat fluxes, which would alter the low-level baroclinicity and, thus, the strength of the underlying synoptic activity that influences the ABSL. In turn, this will allow for a better understanding of not only how the tropics are influencing the warming in West Antarctica and the Antarctic Peninsula but also how these impacts may evolve in the future as ozone recovers and greenhouse gases continue to increase.

[30] **Acknowledgments.** Both authors acknowledge support from the National Science Foundation Office of Polar Programs (grant ANT-0944168). ECMWF is thanked for providing ERA-Int data. Elizabeth Zbacnik is thanked for assistance on investigating the October 1988 event.

References

Bromwich, D. H., J. P. Nicolas, A. J. Monaghan, M. A. Lazzara, L. M. Keller, G. A. Weidner, and A. B. Wilson (2013), Central West Antarctica among the most rapidly warming regions on Earth, *Nat. Geosci.*, *6*, 139–145, doi:10.1038/ngeo1671.

Carvalho, L. M. C., C. Jones, and T. Ambrizzi (2005), Opposite phases of the Antarctic Oscillation and relationships with intraseasonal to interannual activity in the Tropics during the austral summer, *J. Clim.*, *18*, 702–718.

Comiso, J. C. (2010), Variability and trends of the global sea ice cover, in *Sea Ice*, 2nd ed., edited by D. N. Thomas and G. S. Dieckmann, pp. 205–246, Wiley-Blackwell, Oxford.

Dee, D. P., et al. (2011), The ERA-Interim reanalysis: Configuration and performance of the data assimilation system, *Q. J. R. Meteorol. Soc.*, *137*, 553–597.

Ding, Q. H., and E. J. Steig (2013), Temperature change on the Antarctic Peninsula linked to the tropical Pacific, *J. Clim.*, *26*, 7570–7585.

Ding, Q. H., E. J. Steig, D. S. Battisti, and M. Kuttel (2011), Winter warming in West Antarctica caused by central tropical Pacific warming, *Nat. Geosci.*, *4*, 398–403.

Ding, Q. H., E. J. Steig, D. S. Battisti, and J. M. Wallace (2012), Influence of the tropics on the Southern Annular Mode, *J. Clim.*, *25*, 6330–6348.

Fogt, R. L., and D. H. Bromwich (2006), Decadal variability of the ENSO teleconnection to the high latitude South Pacific governed by coupling with the Southern Annular Mode, *J. Clim.*, *19*, 979–997.

Fogt, R. L., D. H. Bromwich, and K. M. Hines (2011), Understanding the SAM influence on the South Pacific ENSO teleconnection, *Clim. Dyn.*, *36*, 1555–1576.

Fogt, R. L., A. J. Wovrosh, R. A. Langen, and I. Simmonds (2012a), The characteristic variability and connection to the underlying synoptic activity of the Amundsen-Bellingshausen Seas Low, *J. Geophys. Res.*, *117*, D07111, doi:10.1029/2011JD017337.

Fogt, R. L., J. M. Jones, and J. Renwick (2012b), Seasonal zonal asymmetries in the Southern Annular Mode and their impact on regional temperature anomalies, *J. Clim.*, *25*, 6253–6270.

Gong, T., S. B. Feldstein, and D. Luo (2010), The impact of ENSO on wave breaking and southern annular mode events, *J. Atmos. Sci.*, *67*, 2854–2870.

Gong, T., S. B. Feldstein, and D. Luo (2013), A simple GCM study on the relationship between ENSO and the Southern Annular Mode, *J. Atmos. Sci.*, *70*, 1821–1832.

Gregory, S., and D. Noone (2008), Variability in the teleconnection between the El Niño–Southern Oscillation and West Antarctic climate deduced from West Antarctic ice core isotope records, *J. Geophys. Res.*, *113*, D17110, doi:10.1029/2007JD009107.

Hio, Y., and S. Yoden (2005), Interannual variations of the seasonal march in the Southern Hemisphere stratosphere for 1979–2002 and characterization of the unprecedented year 2002, *J. Atmos. Sci.*, *62*, 567–580.

Hosking, J. S., A. Orr, G. J. Marshall, J. Turner, and T. Phillips (2013), The influence of the Amundsen-Bellingshausen Seas Low on the climate of West Antarctica and its representation in coupled climate model simulations, *J. Clim.*, *17*, 6633–6648.

Joughin, I., E. Rignot, C. E. Rosanova, B. K. Lucchitta, and J. Bohlander (2003), Timing of recent accelerations of Pine Island Glacier, Antarctica, *Geophys. Res. Lett.*, *30*(13), 1706, doi:10.1029/2003GL017609.

Karoly, D. J. (1989), Southern Hemisphere circulation features associated with El Niño–Southern Oscillation events, *J. Clim.*, *2*, 1239–1252.

Kwok, R., and J. Comiso (2002), Spatial patterns of variability in Antarctic surface temperature: Connections to the Southern Hemisphere Annular Mode and the Southern Oscillation, *Geophys. Res. Lett.*, *29*(14), 1705, doi:10.1029/2002GL015415.

L’Heureux, M. L., and D. W. J. Thompson (2006), Observed relationships between the El-Niño/Southern Oscillation and the extratropical zonal-mean circulation, *J. Clim.*, *19*, 276–287.

Lachlan-Cope, T., and W. Connolley (2006), Teleconnections between the tropical Pacific and the Amundsen-Bellingshausen Seas: Role of the El Niño–Southern Oscillation, *J. Geophys. Res.*, *111*, D23101, doi:10.1029/2005JD006386.

Marshall, G. J. (2003), Trends in the Southern Annular Mode from observations and reanalyses, *J. Clim.*, *16*, 4134–4143.

Marshall, G. J. (2007), Half-century seasonal relationships between the Southern Annular Mode and Antarctic temperatures, *Int. J. Climatol.*, *27*, 373–383.
Marshall, G. J., A. Orr, N. P. M. van Lipzig, and J. C. King (2006), The impact of a changing Southern Hemisphere annular mode on Antarctic Peninsula summer temperatures, *J. Clim.*, *19*, 5388–5404.
Marshall, G. J., S. Di Battista, S. S. Naik, and M. Thamban (2011), Analysis of a regional change in the sign of the SAM-temperature relationship in Antarctica, *Clim. Dyn.*, *36*, 277–287.
Massom, R. A., P. Reid, S. Stammerjohn, S. Barreira, and T. Scambos (2012), Antarctica Sea ice extent and concentration, in State of the Climate in 2011, *Bull. Am. Meteorol. Soc.*, *93*, S154–S155.
Mo, K. C., and W. Higgins (1998), The Pacific–South American modes and tropical convection during the Southern Hemisphere winter, *Mon. Weather Rev.*, *126*, 1581–1596.
Mo, K. C., and J. N. Paegle (2001), The Pacific–South American modes and their downstream effects, *Int. J. Climatol.*, *21*, 1211–1229.
O'Donnell, R., N. Lewis, S. McIntyre, and J. Condon (2011), Improved methods for PCA-based reconstructions: Case study using the Steig et al. (2009) Antarctic temperature reconstruction, *J. Clim.*, *24*, 2099–2115.
Orr, A., G. J. Marshall, J. C. R. Hunt, J. Sommeria, C.-G. Wang, N. P. M. van Lipzig, D. Cresswall, and J. C. King (2008), Characteristics of summer airflow over the Antarctic Peninsula in response to recent strengthening of the westerly circumpolar winds, *J. Atmos. Sci.*, *65*, 1396–1413.
Rignot, E. (2001), Evidence for rapid retreat and mass loss of Thwaites Glacier, West Antarctica, *J. Glaciol.*, *47*, 213–222.
Roscoe, H. K., J. D. Shanklin, and S. R. Colwell (2005), Has the Antarctic vortex split before 2002?, *J. Atmos. Sci.*, *62*, 581–588.
Schneider, D. P., and E. J. Steig (2008), Ice cores record significant 1940s Antarctic warmth related to tropical climate variability, *Proc. Natl. Acad. Sci. U.S.A.*, *105*, 12,154–12,158.
Schneider, D. P., C. Deser, and Y. Okumura (2012a), An assessment and interpretation of the observed warming of West Antarctica in the austral spring, *Clim. Dyn.*, *38*, 323–347.
Schneider, D. P., Y. Okumura, and C. Deser (2012b), Observed Antarctic interannual climate variability and tropical linkages, *J. Clim.*, *25*, 4048–4066.
Silvestri, G. E., and C. S. Vera (2003), Antarctic Oscillation signal on precipitation anomalies over southeastern South America, *Geophys. Res. Lett.*, *30*(21), 2115, doi:10.1029/2003GL018277.
Silvestri, G. E., and C. S. Vera (2009), Nonstationary impacts of the Southern Annular Mode on Southern Hemisphere climate, *J. Clim.*, *22*, 6142–6148.
Stammerjohn, S. E., D. G. Martinson, R. C. Smith, X. Yuan, and D. Rind (2008), Trends in Antarctic annual sea ice retreat and advance and their relation to El Niño Southern Oscillation and Southern Annular Mode variability, *J. Geophys. Res.*, *113*, C03S90, doi:10.1029/2007JC004269.
Stammerjohn, S. E., R. Massom, D. Rind, and D. Martinson (2012), Regions of rapid sea ice change: An inter-hemispheric comparison, *Geophys. Res. Lett.*, *39*, L06501, doi:10.1029/2012GL050874.
Steig, E., D. P. Schneider, S. D. Rutherford, M. E. Mann, J. C. Comiso, and D. T. Shindell (2009), Warming of the Antarctic ice-sheet surface since the 1957 International Geophysical Year, *Nature*, *457*, 459–462.
Steig, E., Q. Ding, D. S. Battisti, and A. Jenkins (2012), Tropical forcing of circumpolar deep water inflow and outlet glacier thinning in the Amundsen Sea Embayment, West Antarctica, *Ann. Glaciol.*, *53*, 19–28, doi:10.3189/2012AoG60A110.
Turner, J. (2004), Review: The El Niño–Southern Oscillation and Antarctica, *Int. J. Climatol.*, *24*, 1–31.
Turner, J., S. R. Colwell, G. J. Marshall, T. A. Lachlan-Cope, A. M. Carleton, P. D. Jones, P. A. Reid, and S. Iagovkina (2004), The SCAR READER project: Toward a high-quality database of mean Antarctic meteorological observations, *J. Clim.*, *17*, 2890–2898.
Turner, J., T. Phillips, J. S. Hosking, G. J. Marshall, and A. Orr (2013), The Amundsen Sea low, *Int. J. Climatol.*, *33*, 1818–1829, doi:10.1002/joc.3558.
Yuan, X. (2004), ENSO-related impacts on Antarctic sea ice: A synthesis of phenomenon and mechanisms, *Antarct. Sci.*, *16*, 415–425.